



# Continuous *in situ* measurements of alkali species in the gasification of biomass

C. Erbel<sup>a,\*<sup>1</sup></sup>, M. Mayerhofer<sup>a,1</sup>, P. Monkhouse<sup>b</sup>, M. Gaderer<sup>a</sup>,  
H. Spliethoff<sup>a,c</sup>

<sup>a</sup> Lehrstuhl für Energiesysteme, Technische Universität München, Garching, Germany

<sup>b</sup> Physikalisch-Chemisches Institut, Universität Heidelberg, Heidelberg, Germany

<sup>c</sup> ZAE Bayern, Abt. 1, Garching, Germany

Available online 29 June 2012

## Abstract

This work describes the first on-line, *in situ* measurement of alkali species in biomass gasification using excimer laser induced fragmentation fluorescence (ELIF). Three pelletised biomass fuels were gasified under different operating conditions in a bubbling fluidized-bed reactor, using steam as the gasifying medium. Concentrations of potassium and sodium were measured in real time for several hours per measurement. Average concentrations obtained for potassium ranged from 140 to 350 ppb, and those for sodium ranged from 1.7 to 60 ppb. Also observed was a slow release of alkali after shutting off the fuel feed, which suggests that alkali species had been taken up in the bed material (olivine); this was confirmed by analysing the bed material before and after use. Consideration of the olivine structure/composition and possible interactions with alkali and other elements during gasification suggests that alkali-containing layers could have formed on the bed particles but appear not to form crystalline phases. This may allow for re-release of alkali while the bed is still hot.

© 2012 Published by Elsevier Inc. on behalf of The Combustion Institute.

**Keywords:** Biomass gasification; Alkali species; In situ measurement; Photofragmentation fluorescence

## 1. Introduction

In the thermal conversion of solid fuels, and particularly of biomass, the hot flue gas is usually contaminated with alkali species in vapour or particulate form. The damage caused to plant materials by such species stems largely from their low melting points and high reactivity. Various plant operational problems have been documented

[1–5], such as abrasion, corrosion, and erosion of system parts, fouling and slagging of heat-transfer surfaces. These problems result in poor heat transfer, plugging of gas-filtering systems as well as restricted usability of ash residuals. Alkali release can also affect the energy and mass flows in boilers and furnaces. If the hot gas from the gasifier/combustor is to be sent directly to a gas turbine, as in combined cycle systems, limits specified by manufacturers for alkali concentrations and particle sizes must be observed to minimize operational problems. Minimum requirements for specific applications are summarised in Ref. [5].

In fluidized-bed (FB) systems, a high level of alkali vaporisation leads to sintering and

\* Corresponding author. Address: Boltzmannstr 15, 85748 Garching, Germany. Fax: +49 89 28916271.

E-mail address: erbel@es.mw.tum.de (C. Erbel).

<sup>1</sup> Both authors contributed equally to this work.

agglomeration of bed material and consequent defluidization [6]. Deposition of alkali compounds can poison and deactivate DeNOx-catalysts [7,8]. Catalyst poisoning is also a problem in feeding hot syngas to SOFCs [9] and MCFCs [10]. On the positive side, though, alkali species are known to catalyse the gasification of char [11].

Thus detailed knowledge on the behaviour of alkali species in plant processes is needed. Obviously the fuel composition plays an important role in determining alkali release. In coal, for example, the water- and mild acid-soluble fractions contain alkali metals in organic structures and simple inorganic salts, whereas the strong acid-soluble fraction holds the mineral-bound alkali metals. Biofuels, in contrast, tend to contain Na and K in accessible, mobile, readily released forms like organic moieties or simple inorganic salts.

To date, the release and fate of alkali species in gasification has been less well investigated than that in combustion and there are few actual measurements of gas-phase alkali concentrations. The only on-line, time-resolved measurements so far under realistic gasification conditions are the following: Most recently, Wellinger et al [12] reported on time-resolved measurements of alkali species by surface ionization (SI) in a wood-fired BFB gasifier and achieved ppb-detection limits. Also detected by SI were alkali species released from single grass pellets in a “mini-gasifier”, a small-scale laboratory device with high temporal resolution though without an absolute calibration [13]. Porbatzki [14] studied alkali release from FB gasification of several biomass fuels, including two wood fuels, on-line by molecular beam mass spectrometry (MBMS). Signals from  $\text{KCl}^+$ ,  $\text{NaCl}^+$ ,  $\text{K}^+$  and  $\text{Na}^+$  were detected, whereby the atomic ions should be fragments of KCl or KOH. Only KCl was calibrated, giving concentrations between 0.1 and 1 ppm.

Prior to the work of Refs. [12–14], alkali measurements were made in the batch mode, usually involving sampling the producer gas for several hours, impingement into washing bottles and off-line flue gas analysis [15–19]. Concentrations measured varied from tens of ppb to tens of ppm, depending on the fuel and whether or not a filter was used or the gas cooled after gasification. Importantly, the batch method provides only *average values* for the time sampled, i.e. peak values are averaged out. Nowadays, continuous on-line monitoring with time resolutions of minutes or less is essential or at least advantageous for alkali control. Filter units, for example, need to be operated in conjunction with on-line measuring devices to verify their effectiveness, especially during plant start-up or on changing the fuel or operating conditions. A real-time measuring system records short-term concentration peaks. In addition, a non-intrusive, optical system dispenses with the need for physical sampling.

So far, there are few continuous, on-line monitoring methods with sufficient robustness for operation in realistic technical environments [20]. As well as MBMS and SI, excimer laser induced fragmentation fluorescence (ELIF) has been applied. Following development at Heidelberg University [20], ELIF has been used extensively for real-time monitoring in the flue gas of solid fuel combustors, e.g. in pulverised [21] and FB combustion of coal [22] and biomass [23]. Alkali species were detected simultaneously in a two-channel system at the respective D-lines, following photofragmentation. During these investigations, alkali species were monitored continuously, non-intrusively and with sub-ppb sensitivity and temporal resolution down to seconds. Also ELIF can be operated to detect gas-phase alkali only, provided the laser energies used are below ca. 10 mJ/cm<sup>2</sup>. This was demonstrated by simultaneous alkali measurements using ELIF and SI [22] and investigating ELIF signals from aerosols in a flame as a function of laser energy density [24].

Independently, sodium species have been detected by ELIF in an atmospheric bench-scale reactor under conditions simulating gasification [25]; a two-wavelength detection scheme allowed discrimination of  $\text{NaCl}$  and  $\text{NaOH}$ . However, alkali detection by ELIF in an actual gasifier has not yet been demonstrated. Predictions of alkali species distributions as a function of temperature for gasification of several biomass fuels have been obtained by equilibrium calculations. Some of these [9,26–32] include woody fuels, others refer to bagasse [29,30] and banagrass [30]. However, such calculations normally only provide the maximum possible quantities of different species as a function of temperature and do not account for effects such as kinetic constraints of specific reactions or capture of alkali by ash or bed particles. Calculations reported in Ref. [9] are for wood gasification using gas data from air-blown and steam gasifiers, respectively, and refer to the temperature interval relevant to SOFCs (750–1000 °C) and for different levels of S, Cl, K and Na. The other calculations mentioned are for air gasification.

The main aim of the current work is the on-line, *in situ* measurement of alkali species in a realistic gasification system, firing three different pelletised fuels in a fluidized bed, atmospheric-pressure reactor. In this way, it was hoped to obtain first direct information on the release of alkali compounds in this type of environment. However, a systematic parametric study has not been performed.

## 2. Experimental

The ELIF method has been described in detail previously [20–23]. Briefly, the method is based on

UV-photofragmentation of alkali molecules present in the flue gas. A broadband excimer laser at 193 nm was used for this purpose; this produces excited alkali atoms in the Na ( $3p\ ^2P$ ) and K ( $4p\ ^2P$ ) states, which then fluoresce at 589 nm and 767 nm, respectively. The present experimental set-up is shown in Fig. 1.

The alkali measurement system is essentially that designed at Heidelberg University and operated for measurements at various locations in Europe [20–23], however with some revisions recently carried out at the TU Munich. First, the hardware-based control unit of the experiment was replaced by a new, programmable real-time data acquisition and control system. The latter additionally evaluates the ELIF signal online, a task hitherto performed post-measurement. The new concept combines several advantages ranging from simplicity and flexibility to real online measurement limited only by the repetition rate of the excimer laser (10 Hz in these experiments). In the course of these modifications, an automatic changing of the neutral density filters could also be implemented, leading to a fully automated system. Second, a universal adjustment device was built based on the previous single-port optical access [33] but enhanced by mechanisms for both alignment of the laser beam and positioning of the glass fibre bundle, which allows for application to arbitrary, even poorly arranged, optical port dimensions and without the need for any constructional modification. Furthermore, the quartz fibre bundle was replaced by a glass fibre bundle of higher numerical aperture. The automated filter wheels and the new glass fibre bundle made it necessary to redesign the optical setup of the detection unit. Great care was taken to reach angle-independent detection efficiency, a prerequisite for quantitative analysis without recalibration for each measurement setup. The changes brought to the ELIF system will soon be reported in more detail elsewhere.

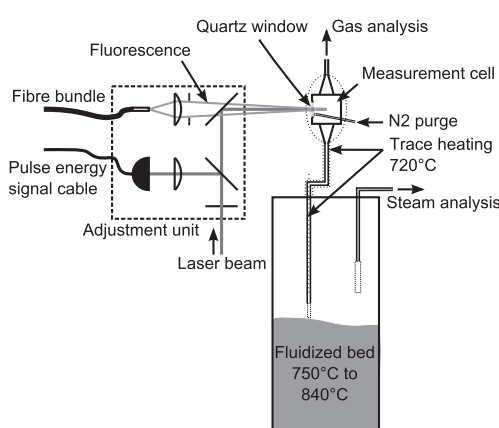


Fig. 1. Experimental setup.

Table 1  
Operational parameters during experiments.

Temperature	750–840	°C
Pressure	0.1–0.2	MPa
S/B	0.75–∞	kg <sub>steam</sub> /kg <sub>fuel</sub>
Fuel input	2–4	kg/h

The reactor employed was a bubbling fluidized bed gasifier, using superheated steam as gasification medium. The reactor vessel (high-temperature resistant steel, i.d.154 mm, length 1500 mm) is designed to work at up to 0.3 MPa and a maximum temperature of 900 °C. The range of the operational parameters in this work is shown in Table 1. The heat required for the endothermic process was provided electrically. The bed material, olivine, had a particle size of 0.1–0.3 mm, the fluidized-bed height was ~600–700 mm throughout the experiments. The biomass pellets were fed with a pressurized screw driver and a drop tube into the bottom of the fluidized bed. The drop tube was flushed with a small nitrogen flow to prevent producer gas and steam from entering the screw driver. The producer gas was cleaned of coarse particles in a cyclone and passed through a ceramic candle filter to remove the fines. After the filter, a valve expanded the producer gas to ambient pressure; most of the gas was then burnt in a combustion chamber. The producer gas cooled rapidly in the freeboard and was too cold for alkali salts to be in the gas phase after the cyclone and the filter (~350 °C). Therefore a slip stream was taken directly from the freeboard, kept at >700 °C and channelled into the optical port for the ELIF measurement. The optical measurement cell was kept at ~730 °C throughout the experiments. The dry gas

Table 2  
Chemical composition of biomasses (dry) (%).

	Agrol	Willow	DDGS
Al	<0.005	0.037	<0.005
Ba	0.001	0.001	<0.001
Ca	0.078	0.470	0.100
Fe	0.004	0.034	0.012
K	0.044	0.250	1.760
Mg	0.017	0.049	0.300
Mn	0.012	0.007	0.007
Na	0.008	0.021	0.350
Si	0.009	0.220	0.053
Ti	0.020	0.012	<0.002
C	51.0	50.3	48.2
Cl	0.005	0.007	0.210
S	<0.002	<0.002	0.755
O	38.2	37.4	31.2
N	0.15	0.69	5.52
H	6.26	6.17	6.54
Water (%)	8.00	8.00	12.00
Ash (%)	0.144	2.517	4.822

Table 3  
Chemical composition of biomass ashes (%).

	Agrol	Willow	DDGS
Al <sub>2</sub> O <sub>3</sub>	2.683	4.232	0.051
BaO	0.413	0.063	0.015
CaO	33.301	26.305	2.868
Fe <sub>2</sub> O <sub>3</sub>	1.315	1.544	0.257
K <sub>2</sub> O	16.503	13.130	38.066
MgO	7.794	2.885	8.872
MnO	3.964	0.297	0.155
Na <sub>2</sub> O	0.998	1.672	10.042
SiO <sub>2</sub>	6.461	33.802	1.861
TiO <sub>2</sub>	0.060	0.184	-
C	5.240	3.610	0.332
Cl	0.067	0.110	0.018
SO <sub>3</sub>	2.457	2.272	10.038

composition (H<sub>2</sub>, CO, CO<sub>2</sub> and CH<sub>4</sub>) was monitored after the measurement cell using a gas analyser. The steam content of the gas was measured by a psychrometer in another slip stream, also taken directly from the gasifier freeboard.

*Analysis of fuels and bed material:* Elemental and ash analyses for the three pelletised fuels used (Agrol = mixture of 80% spruce + 20% pine; Willow; DDGS = dried distillers' grains with solubles, a cereal byproduct obtained during the distillation process) are shown in Tables 2 and 3. The main inorganic components of the three fuels were analysed by ICP-OES, with a detection limit of  $\leq 0.005$  wt%.

Analysis of the olivine bed material before use gave the composition 42% SiO<sub>2</sub>, 9.8% Fe<sub>2</sub>O<sub>3</sub>, 46.7% MgO, 0.1% CaO, 0.4% Al<sub>2</sub>O<sub>3</sub>.

### 3. Results and discussion

#### 3.1. Evaluation procedure

If radiation trapping is negligible and the laser fluence is small as mentioned later in this section, the expectation value of the raw ELIF signal  $\langle S_M \rangle$  ( $M \in \{\text{Na, K}\}$ ) is related to the number densities of the respective gas-phase alkali compounds  $\rho_{MX}$  ( $X \in \{\text{Cl, OH, ...}\}$ ) as follows:

$$\begin{aligned} \langle S_M \rangle &= c_0 \cdot E \cdot \hat{g} \cdot \sum_{X \in \{\text{Cl, OH}\}} \rho_{MX} \cdot a_{MX} \cdot q_{MX} \\ &\quad + \langle S_M^h \rangle + \langle S_M^0 \rangle \end{aligned} \quad (1)$$

with  $c_0$  a constant,  $E$  the laser pulse energy,  $a_{MX}$  the cross section for excitation of  $MX$ ,  $q_{MX}$  the corresponding quenching factor,  $\langle S_M^h \rangle$  and  $\langle S_M^0 \rangle$  offsets due to thermal background and self-fluorescence of the measurement apparatus, respectively, and  $\hat{g}$  a weighted geometric factor. The latter factor accounts for both the dimensions of the fluorescence volume and the laser beam absorption by foreign gases. It is defined as

$$\hat{g} := \int_{x_1}^{x_2} dx \cdot A(x) \cdot T(x), \quad (2)$$

where  $x_1$ ,  $x_2$  denote the limits of the fluorescence volume,  $A(x)$  the fluorescence collection efficiency and  $T(x)$  the relative transmission of the laser radiation.

In the current experiments, the gas-phase alkali species were chlorides and hydroxides; other species such as sulphates, carbonates and oxides are not present under our physical and chemical conditions. (The formation and transformation pathways of alkali species are discussed below in Section 3.) The absorption cross sections for sodium chloride and sodium hydroxide are known to be similar [34,35]. In the case of potassium, data are insufficient, but the corresponding values can be expected to be similar also. With this information ( $a_M := a_{MX}$ ) and assuming a thermal distribution of the velocities of the excited alkali atoms ( $q_M := q_{MX}$ ) [36] rearrangement of Eq. (1) yields

$$\rho_M = \frac{\langle S_M - S_M^h \rangle - \langle S_M^0 \rangle}{c_M \cdot E \cdot \hat{g} \cdot q_M}, \quad (3)$$

with  $\rho_M := \sum_{X \in \{\text{Cl, OH, ...}\}} \rho_{MX}$  the number density of gas-phase compounds of  $M$  and  $c_M := c_0 a_M$  the corresponding calibration factor.

As for the other requirements, the gas-phase alkali concentrations are well below typical thresholds where radiation trapping occurs [37] and the laser fluence is always kept below 10 mJ/cm<sup>2</sup>, thus ensuring that only gas-phase alkali species are detected [22,24].

The calibration factors  $c_M$  were obtained by measuring ELIF signals in an evacuated reference cell, where defined gas-phase alkali chloride number densities were generated by sublimation of the respective solids. The setup was essentially the same as that described earlier [36,38]. The quenching factors and the laser beam absorption were calculated from the respective cross sections [20,36] and measured data for the gas composition, pressure and temperature in the measurement cell. The ELIF data were averaged online using an exponential moving average with a time constant of 5 s (10 s in the Agrol measurement) and, simultaneously the corresponding (moving) measurement uncertainties were determined. Finally, the number densities were converted into partial pressures, assuming an ideal gas, and the volume fractions of potassium and sodium species in the reactor gas were computed, respectively.

#### 3.2. Average gas-phase alkali concentrations and time profiles during gasification

First, Fig. 2a and b present average sodium and potassium concentrations for the different feedstocks, respectively. The operational parame-

ters were 800 °C, S/B 1/1 and atmospheric pressure (only for DDGS the steam to biomass (S/B) ratio was 1.25/1) and are standard values. The bars represent the standard deviations of the respective underlying profiles, which are mainly attributed to uncertainties in operational parameters and feedstock inhomogeneity. The results show that the alkali concentration in the feedstock has a strong influence on alkali release, however – at least under these operating conditions – the dependence is not proportional. For example, the potassium content in DDGS fuel is 40 times higher than in Agrol fuel, (see Table 2) but the potassium gas-phase concentration is only 2.2 times higher.

The influence of reactor temperature, pressure and S/B variations was also investigated. The range of operational parameters is given in Table 1. Figures 3–6 show exemplary time profiles. The steam measurement device occasionally failed due to filter blockage by particles. Because during these periods the H<sub>2</sub>O partial pressures are not available, complete evaluation of the ELIF signal is not possible leading to gaps in

the concentration profiles. For both sodium and potassium typical fractional standard errors of the mean values were about 7%, except for the very low sodium concentrations shown in Fig. 5 (Agrol), where they amounted to 26%.

During most measurements, there were no significant variations in bed temperature. However in the measurement using Willow fuel (Fig. 3), some variations did occur. The alkali concentrations do not appear to react significantly to the fall in temperature under the standard conditions. This result may be associated with the relative rates of release/capture of alkali by minerals in the ash or the bed. Also, careful analysis of the setup shows that it is not due to resublimation in the sample line, which would otherwise “cut off” measurable concentrations. Figure 4 shows a profile where the potassium concentration falls as the pressure rises. Such a response was predicted by Gabra et al. [29] for chlorides in bagasse gasification, but was not discussed further. One possibility would be formation of species such as (particulate) sulphates [39], which are not detectable by ELIF.

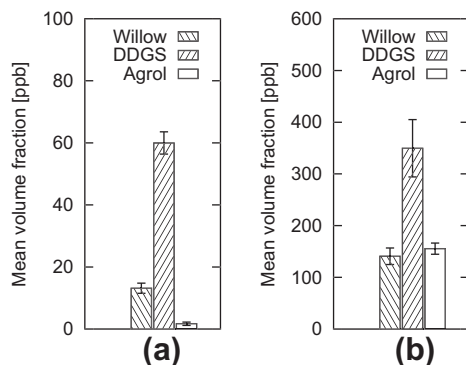


Fig. 2. Average sodium (a) and potassium (b) concentrations in the producer gas at standard operating conditions.

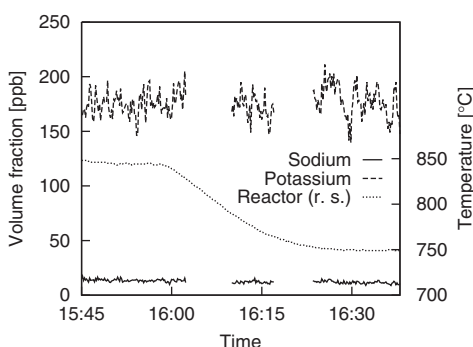


Fig. 3. Alkali concentrations and bed temperature (Willow). “r.s.” refers to “right scale”.

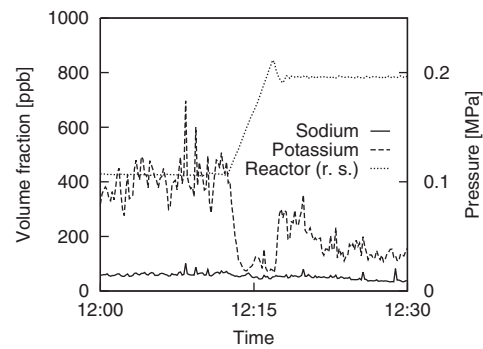


Fig. 4. Alkali concentrations and reactor pressure (DDGS). “r.s.” refers to “right scale”.

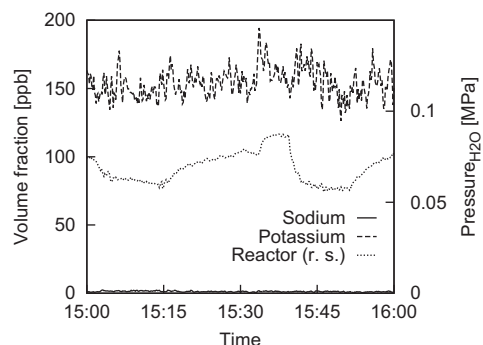


Fig. 5. Alkali concentrations and steam partial pressure (Agrol). “r.s.” refers to “right scale”.

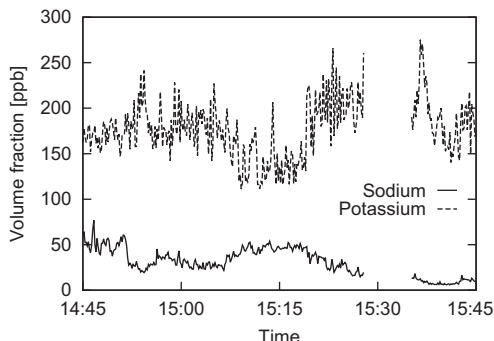


Fig. 6. Alkali concentrations (first Agrol measurement).

Figure 5 shows a short-term variation of the S/B ratio where the partial pressure of steam inside the gasification reactor is plotted against gas-phase alkali concentrations. No significant correlation can be observed, which suggests that the release of alkali in hydroxide form is not limited by the amount of steam. During the same measurement, the fuel input was completely switched off from 15:32 to 15:39 h but this had no effect on alkali gas phase concentrations either. This suggests that the summed bed particle surface acts as a huge buffer, taking up the greater part of the alkali species before re-release. Thus the amount of alkalis released from the bed is many times higher than that released by the fuel directly. Indeed, analysis of the bed material after the measurement series showed the presence of considerable amounts of alkalis, in contrast to the unused olivine (Table 4). For this purpose the bed material (olivine-charcoal mixture) was removed from the reactor, sieved and separated into three main fractions: fine charcoal, of average particle size less than that of olivine (0.23 mm); rough charcoal (of particle size significantly larger than that of olivine (2–5 mm)) and a fraction that most likely corresponds to the used olivine. All three fractions were analysed by AAS.

Figure 6 shows alkali concentrations during an Agrol measurement, where a slowly decreasing release of sodium over a period of one hour can be seen. This arises from an initially high contamination of the bed with sodium species from the DDGS measurement, which was done just prior to this Agrol measurement. Retention of alkali in the bed had been observed previously in ELIF alkali measurements at an FBC-reactor [40], in

Table 4  
Analysis of charcoal/bed material.

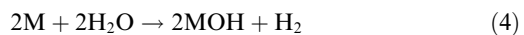
	Na <sub>2</sub> O (%)	K <sub>2</sub> O (%)
Unused olivine	0.00	0.00
Fine charcoal	0.10	0.30
Rough charcoal	0.18	0.93
Used olivine	0.14	0.71

cases where the fuel contained high amounts of chlorine. A discussion of the interaction of alkali with the bed material will be found below in Section 3.2.

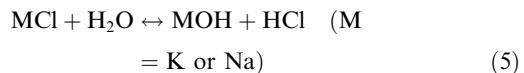
### 3.3. Alkali transformations under gasification conditions

#### 3.3.1. Gas- and condensed phase chemistry

Depending on the extent of drying in the fuel, some alkali may be present dissolved in the water content and this should volatilise as NaOH in the gas phase [41,42]. For low Cl/(Na + K) ratios (the case for Agrol and Willow fuels) however, initial volatilization of alkali should occur in elemental form by dissociation of alkali bonded to the carbonaceous part of the char or fuel, e.g., in carboxylic form C–O–O–M<sup>+</sup> [43], where C represents carbon of the char/fuel matrix and M is Na or K. The alkali atoms formed then react with steam in the gasification system:

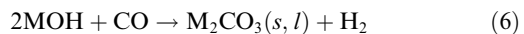


The low amounts of chlorine in the fuels Agrol and Willow and the high water vapour content of the gasifier will shift reaction (2) towards the product side [9,44]:



For decreasing temperatures and increasing hydroxide (or HCl) concentration though, this equilibrium will tend back to the educt side.

The hydroxide formed in reactions (1) and (2) can also react with CO in the flue gas:



Sodium carbonate is normally solid up to 851 °C, but in steam, the melting point falls to between 800 and 750 °C [40]. By 900 °C, the carbonates of both alkalis should evaporate completely [9]. However, even if present, these species would not be in gaseous form at the temperature (730 °C) of the ELIF-measurement.

In contrast to the other two fuels tested, DDGS contains high amounts of sulphur and chlorine. Thus the quantity and proportion of chlorides formed initially should be much higher, but again the high level of steam will still shift reaction (2) towards the hydroxides. Sulphur chemistry will also play some role although there should be no sulphate in the gas phase. Calculations for steam gasification of lignite [45] and for wood gasification [9] predict small amounts of the condensed sulphides Na<sub>2</sub>S(l) and K<sub>2</sub>S(l) between 750 and 900 °C.

#### 3.3.2. Role of bed material

The interaction of fuel components with bed material has been studied by a number of authors,

both theoretically and experimentally [30,46–51]. Bed material analyses generally show that a significant part of the alkali from the fuel is taken up in the bed, but the amount and rate of uptake and the chemistry involved depends on the nature and size of bed particles, free-board velocities as well as the chemical composition of the fuel and of the bed.

**Table 4** shows that the three fractions of material taken from the gasifier after the measurements contain Na and K in different amounts. In particular, the third fraction, which probably corresponds closest to the post-test olivine, contains 0.71% K<sub>2</sub>O and 0.14% Na<sub>2</sub>O, whereas the fresh olivine contained no alkali. So clearly uptake of alkali into the bed had occurred, but further information is needed to establish what kind of interaction has taken place and in what form the captured alkali is present.

First, the different crystal structures and phase diagrams of olivine and silica should be noted: that of olivine is orthorhombic and is stable up to the melting point (ca. 1750 °C), forming a continuous solid solution. In contrast, quartz changes its form with temperature [52]. Indeed, the crystal structure and its temperature behaviour is likely to influence the reactivity (and hence adhesion and agglomeration tendency) of the bed material significantly.

Some important clues about the behaviour of olivine in thermal conversion processes can be gained from previous investigations. In the study of Davidsson et al. [46], for example, the effects of different bed materials, including quartz sand and olivine, were studied during the CFB combustion of wood/straw mixtures. The interaction of the fuel with the bed (here manifested by the tendency of bed particles to adhere and agglomerate) was much less for the olivine case. Indeed, although alkali was captured by the bed, it did not react with the olivine particles. Instead, alkali was seen in thick layers on and between other bed particles. The detailed work of Zevenhoven-Onderwater et al. [28,47] shows that the formation of silicate melt, which is believed to be responsible for the adhesion between particles, was much reduced when changing the bed from silica to olivine or another low-silica bed material. Similarly, a recent study on changes to olivine bed material in steam gasification of woody biomass [51] revealed that the inner coating of the bed particles consists of calcium silicate and that K is present in the outer coating.

Finally, although a direct reaction of gaseous K with the olivine surface to form mixed silicates of K and Mg is theoretically possible [53] there is so far no clear experimental evidence for this. In fact, the XRD results for both unused and used olivine in Ref. [51] show crystalline phases containing Mg, Ca and Fe, but none of potassium. Thus one can only assume that K is taken up in

some other form as a result of the high volatile content of K in the fuel.

In any case, incorporation of the alkaline earths Mg and Ca (present in large amounts in the Agrol and Willow fuels) into the relatively tightly layered crystal structure of olivine is more probable than that of the larger K and Na atoms [54], so low-melting alkali silicates are less likely to be formed than with a high-quartz bed material.

Considering all these studies, the observed slow release of alkali after shutting off the fuel feed suggests that layers could have formed on the bed particles but that alkali should be present on the outer layer thereof. This may allow for re-release of alkali, provided that the temperature remains at a sufficiently high level.

#### 4. Conclusions

In this work we have demonstrated for the first time the capability of the ELIF method to measure continuously gaseous alkali concentrations under realistic gasification conditions. Three different types of pelletized biomass were gasified under near-atmospheric pressure conditions. In all cases, the greater part of the fuel alkali is found to be taken up in the bed during gasification. However, alkali species are gradually re-released from the bed after shutting off the fuel supply, suggesting that a non-permanent (outer) coating had been formed on the bed particles. However, further systematic work, preferably a parametric study, is needed to verify the exact interaction and form of alkali on the bed.

#### Acknowledgements

This work was carried out in the frame of the EU project GreenSyngas (Project number 213628). This work was also supported by the Federal Ministry for the economy and technology as well as industrial partners (Siemens, RWE, EnBW, Vattenfall, E.ON) under project HotVeGAs (Contract no. 0327773A). The provision of fuel analyses from the Forschungszentrum Jülich (M. Ryš, H. Lippert, M. Müller) is also gratefully acknowledged. Lantmannen (Sweden) is gratefully acknowledged for providing biomass feedstock.

#### References

- [1] R.W. Bryers, *Prog. Energy Combust. Sci.* 22 (1996) 29–120.
- [2] M.E.C. Forster, *Int. J. Energy Technol. Policy* 5 (3) (2007) 383–390.
- [3] A.A. Khan, W. de Jong, P.J. Jansens, H. Spliethoff, *Fuel Proc. Technol.* 90 (2009) 21–50.

- [4] R. Beining, M. Adelt, A. Vogel, *Chem. Ing. Tech.* 82 (2010) 1941–1953.
- [5] M. Rodrigues, W.A. Arnaldo, A.P.C. Faaij, *Energy Convers. Manage.* 48 (2007) 1289–1301.
- [6] M. Bartels, W. Lin, J. Nijenhuis, F. Kapteijn, J.R. van Ommen, *Prog. Energy Combust. Sci.* 34 (2008) 633–666.
- [7] A.-C. Larsson, J. Einvall, M. Sanati, *Aerosol. Sci. Technol.* 41 (4) (2007) 369–379.
- [8] A.K. Neyestanaki, F. Klingstedt, T. Salmi, D.Y. Murzin, *Fuel* 83 (4–5) (2004) 395–408.
- [9] A. Norheim, D. Lindberg, J.E. Hustad, R. Backman, *Energy Fuels* 23 (2009) 920–925.
- [10] C. Tomasi, M. Barattieri, B. Bosio, E. Arato, P. Baggio, *J. Power Sources* 157 (2) (2006) 765–774.
- [11] C.-Z. Li, *Fuel* 86 (2007) 1664–1683.
- [12] M. Wellinger, S. Biollaz, J. Wochele, C. Ludwig, *Energy Fuels* 25 (9) (2011) 4163–4171.
- [13] J. Judex, *Grass for Power Generation*, Ph.D. thesis, ETH Zürich, 2010, Chapter 5.
- [14] D. Porbatzki, *Freisetzung anorganischer Spezies bei der thermochemischen Umwandlung biogener Festbrennstoffe*, Ph.D. thesis, RWTH Aachen, 2008.
- [15] S.Q. Turn, C.M. Kinoshita, D.M. Ishimura, T.T. Hiraki, J. Zhou, *Fuel* 77 (3) (1998) 135–146.
- [16] S.Q. Turn, C.M. Kinoshita, D.M. Ishimura, T.T. Hiraki, J. Zhou, S.M. Masutani, *Ind. Eng. Chem. Res.* 40 (2001) 1960–1967.
- [17] S.V.B. Van Paasen, M.K. Cieplik, N. Phokawat, *Gasification of Non-Woody Biomass*, Report ECN-C-06-032, Energy Research Centre of the Netherlands, 2006.
- [18] K. Salo, W. Mojtabedi, *Biomass Bioenergy* 15 (3) (1998) 263–267.
- [19] J. Smeenk, R.C. Brown, D. Eckels, Proceedings of the 4th Biomass Conference of the Americas, Oakland, CA, USA, 1999, vol. 2, pp. 961–967.
- [20] P. Monkhouse, *Prog. Energy Combust. Sci.* 37 (2011) 125 and 28 (2002) 331–381.
- [21] H. Schürmann, P.B. Monkhouse, S. Unterberger, K.R.G. Hein, *Proc. Combust. Inst.* 31 (2007) 1913–1920.
- [22] P.B. Monkhouse, U.A. Gottwald, K.O. Davidsson, B. Lönn, K. Engvall, J.B.C. Pettersson, *Fuel* 82 (2003) 365–371.
- [23] M. Glazer, M.P. Khan, H. Schürmann, P. Monkhouse, W. de Jong, H. Spliethoff, *Energy Fuels* 19 (2005) 1889–1897.
- [24] M. Hidalgo Nuñez, N. Omenetto, *Appl. Spectrosc.* 55 (2001) 809–951.
- [25] B. Chadwick, G. Domazetis, R.J.S. Morrison, *Anal. Chem.* 67 (1995) 710–716.
- [26] M. Stemmller, *Chemische Heißgasreinigung bei Biomassevergasungsprozessen*, Ph.D. thesis, RWTH Aachen, 2010.
- [27] X. Wei, U. Schnell, K.R.G. Hein, *Fuel* 84 (2005) 841–848.
- [28] M. Zevenhoven-Onderwater, R. Backman, B.-J. Skrifvars, M. Hupa, *Fuel* 80 (2001) 1489–1502.
- [29] M. Gabra, A. Nordin, M. Öhman, B. Kjellström, *Biomass Bioenergy* 21 (2001) 461–476.
- [30] S.Q. Turn, *Ind. Eng. Chem. Res.* 46 (2007) 8928–8937.
- [31] Värnamo Project, available at lnu.se/polopoly\_fs/1.3304!chrisgas\_folder\_07\_v5.pdf, accessed 19.12.11.
- [32] Güssing Project, available at www.uniqueproject.eu, accessed 19.12.11.
- [33] U. Gottwald, P. Monkhouse, *Appl. Phys. B* 69 (1999) 151–154.
- [34] D. Self, J. Plane, *Phys. Chem. Chem. Phys.* 4 (2002) 16–23.
- [35] J.A. Silver, D.R. Worsnop, A. Freedman, C. Kolb, *Chem. Phys.* 84 (8) (1986) 4378–4384.
- [36] K. Hartinger, S. Nord, P. Monkhouse, *Appl. Phys. B* 64 (1997) 363–367.
- [37] B. Chadwick, R.J. Morrison, *J. Chem. Soc. Faraday Trans.* 91 (1995) 1931–1934.
- [38] R. Oldenborg, S. Baughcum, *Anal. Chem.* 58 (1986) 1430–1436.
- [39] L. Hindiyarti, F. Frandsen, H. Livbjerg, P. Glarborg, P. Marshall, *Fuel* 87 (2008) 1591–1600.
- [40] U. Gottwald, P. Monkhouse, N. Vulgaris, B. Bonn, *Fuel Proc. Technol.* 75 (2002) 215–226.
- [41] H.M. Westberg, M. Byström, B. Leckner, *Energy Fuels* 17 (2003) 18–28.
- [42] J. Werkelin, B.-J. Skrifvars, M. Zevenhoven, B. Holmbom, M. Hupa, *Fuel* 89 (2010) 481–493.
- [43] T. Okuno, N. Sonoyama, J.-I. Hayashi, C.-Z. Li, *Energy Fuels* 19 (2005) 2164–2171.
- [44] D.C. Dayton, R.J. French, T.A. Milne, *Energy Fuels* 9 (1995) 855–865.
- [45] A. Kosminski, D.P. Ross, J.B. Agnew, *Fuel Proc. Technol.* 87 (2006) 953–962, 1037–1049.
- [46] K.O. Davidsson, L.E. Åmand, B.M. Steenari, A.-L. Elled, D. Eskilsson, B. Leckner, *Chem. Eng. Sci.* 63 (2008) 5314–5329.
- [47] M. Zevenhoven-Onderwater, R. Backman, B.-J. Skrifvars, et al., *Fuel* 80 (2001) 1502–1512.
- [48] S. De Geyter, M. Öhmann, D. Boström, M. Eriksson, A. Nordin, *Energy Fuels* 21 (2007) 2663–2668.
- [49] L.H. Nuutinen, M.S. Tiainen, M.E. Virtanen, S.H. Enestam, R.S. Laitinen, *Energy Fuels* 18 (2004) 128–130.
- [50] M. Öhman, L. Pommer, A. Nordin, *Energy Fuels* 19 (2005) 1742–1748.
- [51] F. Kirnbauer, H. Hofbauer, *Energy Fuels* 25 (8) (2011) 3793–3798.
- [52] Available at <http://www.minerals.net/Mineral-Main.aspx>, accessed 19.12.11.
- [53] E.W. Roedder, *J. Am. Sci.* 249 (1951) 97–130.
- [54] P. Thy, C.E. Lesher, B.M. Jenkins, *Fuel* 79 (2000) 693–700.